Available online at www.sciencedirect.com
SCIENCE DIRECT®
Physics of the Earth and Planetary Interiors 149 (2005) 187–200
PHYSICS OF THE EARTH AND PLANETARY INTERIORS
www.elsevier.com/locate/pepi

Thermal structure of the Costa Rica – Nicaragua subduction zone

Simon M. Peacock[a,*], Peter E. van Keken[b], Stephen D. Holloway[c], Bradley R. Hacker[d], Geoffrey A. Abers[e], Robin L. Fergason[a]

[a] *Department of Geological Sciences, Box 871404, Arizona State University, Tempe, AZ 85287-1404, USA*
[b] *Department of Geological Sciences, University of Michigan, Ann Arbor, MI, USA*
[c] *Department of Geological Sciences, University of Texas El Paso, El Paso, TX, USA*
[d] *Department of Geological Sciences, University Calif. Santa Barbara, Santa Barbara, CA, USA*
[e] *Department of Earth Sciences, Boston University, Boston, MA, USA*

Received 5 March 2004; received in revised form 2 July 2004; accepted 26 August 2004

Abstract

We constructed four high-resolution, finite-element thermal models across the Nicaragua – Costa Rica subduction zone to predict the (i) thermal structure, (ii) metamorphic pressure (P)–temperature (T) paths followed by subducting lithosphere, and (iii) loci and types of slab dehydration reactions. These new models incorporate a temperature- and stress-dependent olivine rheology for the mantle–wedge that focuses hot asthenosphere into the tip of the mantle–wedge. At $P = 3$ GPa (100 km depth), predicted slab interface temperatures are ∼800 °C, about 170 °C warmer than temperatures predicted using an isoviscous mantle–wedge rheology. At the same pressure, predicted temperatures at the base of 7 km thick subducting oceanic crust range from 500 °C beneath SE Costa Rica to 400–440 °C beneath Nicaragua and NW Costa Rica. The high thermal gradients perpendicular to the slab interface permit partial melting of subducting sediments while the underlying oceanic crust dehydrates, consistent with recent geochemical studies of arc basalts. Hydrous eclogite is predicted to persist to ∼120 km depth beneath Nicaragua. This is slightly less than the ∼150 km depth extent of a dipping low-seismic-velocity wave guide which may reflect deeper persistence of metastable gabbro. Along-strike variations in the calculated thermal structure are relatively minor compared to variations in the distribution of Wadati-Benioff earthquakes and arc geochemistry, suggesting that regional variations in slab stresses, crustal thickness, incoming sediment load, and the distribution of hydrous minerals in the incoming lithosphere play important roles.

Keywords: Subduction; Thermal modelling; Metamorphism; Arc magmatism; Lithosphere

1. Introduction

Earthquakes and arc magmatism in subduction zones are intimately related to the thermal structure

* Corresponding author. Tel.: +1 480 965 3391; fax: +1 480 965 1093.
E-mail address: peacock@asu.edu (S.M. Peacock).

0031-9201/$ – see front matter © 2004 Elsevier B.V. All rights reserved.
doi:10.1016/j.pepi.2004.08.030

of the subducting plate and overlying mantle–wedge. Rates of subduction are more rapid than rates of thermal diffusion such that the cold core of subducting plates may be up to 1000 °C cooler than the surrounding mantle. Variations in the subduction rate and the age of incoming oceanic lithosphere lead to considerable variations in the thermal structure of different subduction zones. Rapid subduction of mature oceanic lithosphere (e.g., NE Japan, Izu-Bonin) results in subducting plates that are ∼300 °C cooler than subduction zones characterized by modest convergence and young incoming lithosphere (e.g., SW Japan, Cascadia) (Peacock and Wang, 1999). Cooler subducting plates correlate with deeper Wadati-Benioff seismicity and more vigorous arc magmatism (e.g., Kirby et al., 1996; Peacock and Wang, 1999; Hacker et al., 2003b).

The Central American subduction zone is characterized by rapid (70–90 mm/year) convergence of young (15–25 Ma) oceanic lithosphere (Barckhausen et al., 2001; DeMets, 2001). Temperatures within the subducting Cocos plate should therefore lie between the cool (NE Japan) and warm (SW Japan) end-member subduction zones. In the Central American subduction zone both the convergence rate and the age of the incoming lithosphere vary only slightly along-strike, but there are dramatic along-strike changes in the depth of Wadati-Benioff seismicity (Protti et al., 1995), position of the volcanic front, and arc geochemistry (Carr et al., 1990; Leeman et al., 1994; Herrstrom et al., 1995). The Costa Rica – Nicaragua segment of the Central American subduction zone is as a focus site for two National Science Foundation Margins initiatives: the Seismogenic Zone Experiment (SEIZE) and the Subduction Factory.

2. Geotectonic setting

The Cocos plate subducts northeastward beneath the Caribbean plate along the Middle America trench (Fig. 1). The convergence rate between the Cocos and Caribbean plates increases to the southeast, from ∼60 mm/year off southern Guatamala to ∼90 mm/year off southern Costa Rica (DeMets, 2001). Convergence is oblique, partitioned such that the forearc translates to the northwest at 10–15 mm/year (DeMets, 2001; Norabuena et al., submitted for publication). Along this margin, large subduction-thrust earthquakes have ruptured the Cocos – Caribbean plate interface. Deeper earthquakes define a Wadati-Benioff zone that marks the subducting Cocos plate and extends to 250 km depth beneath Nicaragua (Protti et al., 1995; Husen et al., 2003). A 1500 km-long volcanic arc extends from southern Mexico to central Costa Rica, but there is no Holocene volcanism in southern Costa Rica (e.g., Carr et al., 1990; Leeman et al., 1994).

The Cocos plate formed at two different spreading centers – the Cocos–Pacific spreading center (i.e., the east pacific rise, EPR) and the Cocos–Nazca spreading center (CNS) (von Huene et al., 1995; Barckhausen et al., 2001). Northwest of the Nicoya peninsula in NE Costa Rica, relatively smooth Cocos crust, created at the rapid-spreading EPR, is being subducted. That sea floor is characterized by extensive trench-parallel grabens forming just seaward of the trench (Ranero et al., 2003). Southeast of the Nicoya peninsula, relatively rough Cocos crust created at the slow-spreading CNS, is being subducted. Abundant seamounts roughen the crust here, and deform the forearc wedge where they collide (von Huene et al., 2000). The age of the Cocos plate at the Middle America trench decreases towards the southeast, from 24 Ma off Nicaragua to 15 Ma off SE Costa Rica.

Offshore of southern Costa Rica, the NE-trending Cocos Ridge represents the trace of the Galapagos hot spot. The thickness of the Cocos crust increases towards the southeast, from 5 to 7 km off Nicaragua to 12 km off SE Costa Rica on the flank of the Cocos Ridge (von Huene et al., 2000) to 21 km along the thickest part of the Cocos Ridge off SE Costa Rica (Walther et al., 2000). Subduction of this aseismic ridge coincides with the abrupt shallowing of slab seismicity and SE cessation of volcanism.

Conductive cooling calculations predict that the heat flow through the surface of 15–25 Ma oceanic lithosphere should be 100–130 mW/m^2. The sea floor generated at the EPR shows anomalously low values of 20–40 mW/m^2, while that generated at the CNS generates 105–115 mW/m^2 (Fisher et al., 2003). Off the Nicoya peninsula, Langseth and Silver (1996) measured heat flow values of 12 mW/m^2 outboard of the trench and 17 mW/m^2 on the trench floor. These exceptionally low heat flow values are best explained by vigorous hydrothermal circulation in the uppermost crust (Langseth and Silver, 1996; Fisher et al., 2003).

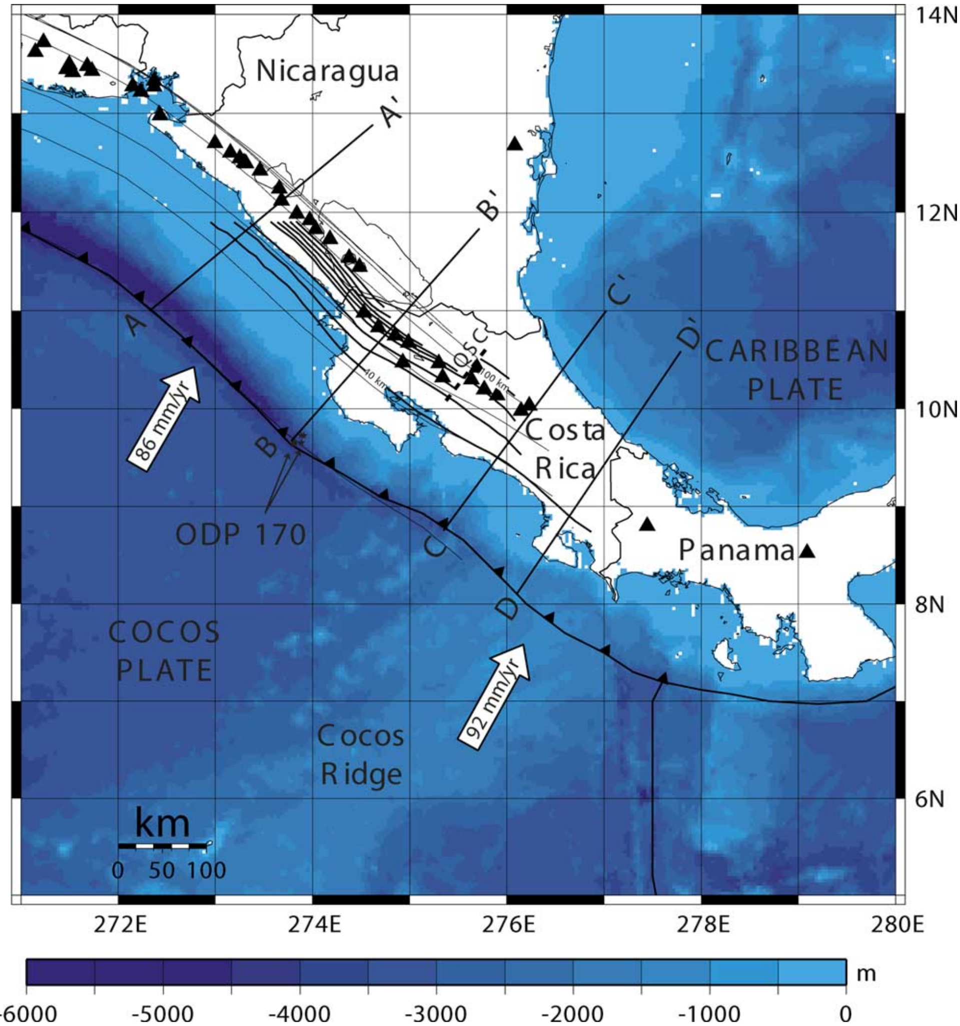

Fig. 1. Geotectonic map of Central America showing location of four transects for which thermal models were constructed. A–A′, Nicaragua transect; B–B′, NW Costa Rica transect; C–C′, Central Costa Rica transect; D–D′, SE Costa Rica transect. Solid triangles: Holocene volcanoes; thin lines: depth to Wadati-Benioff seismicity (Protti et al., 1995); QSC, Quesada sharp contortion (Protti et al., 1995). ODP 170, Oceanic Drilling Program Leg 170 drill sites 1039–1043.

The Costa Rica – Nicaragua subduction zone is a non-accreting margin characterized by a very small frontal prism and subduction erosion (von Huene and Scholl, 1991; Ranero and von Huene, 2000; von Huene et al., 2000). Off the Nicoya peninsula, analysis of ODP sites 1040 and 1043 reveals that all 400 m of marine sediments on the incoming Cocos plate are being subducted beneath the toe of the frontal prism (Silver, 2000; Kimura et al., 1997). Uniformly low ^{10}Be concentrations in prism sediments at ODP site 1040 indicate that no frontal accretion has occurred for at least the past 3–4 million years (Morris et al., 2002).

Wadati-Benioff zone seismicity defines a complex geometry for the subducting Cocos plate. Fig. 2 shows seismicity from within 25 km on either side of the profiles A–A′ through D–D′ from Fig. 1. The seismicity is based on regional observations from deployments in Costa Rica (Protti et al., 1995; Newman et al., 2002; DeShon et al., 2003) and the EHB teleseismic catalogue (Engdahl et al., 1998). The solid lines indicate

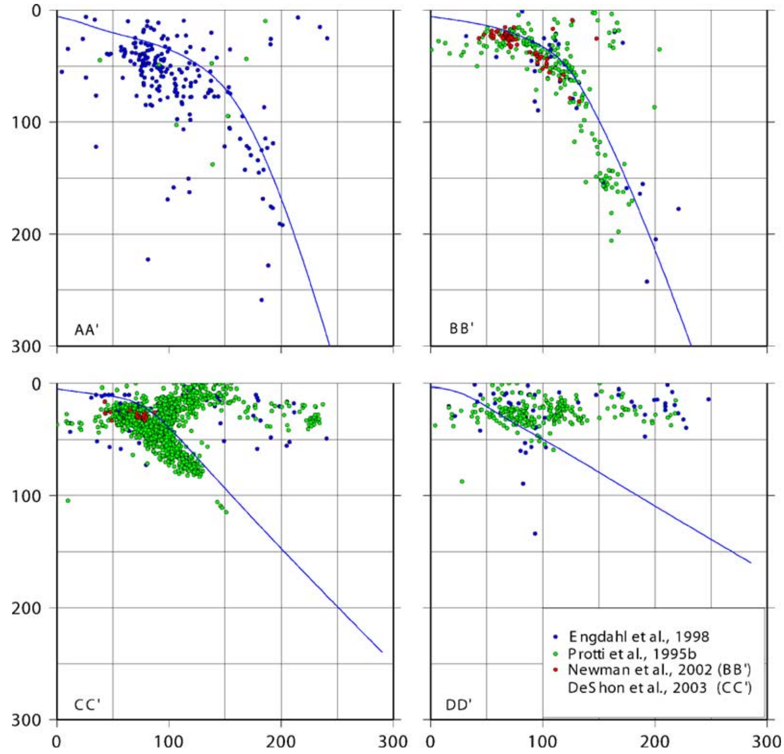

Fig. 2. Seismicity (symbols) and inferred slab surface geometry (solid lines). We plot events larger than magnitude 2.5 from up to 25 km away from the each profile. Seismicity is based on the EHB teleseismic catalogue (blue circles) and three regional experiments (Protti et al., 1995; Newman et al., 2002; DeShon et al., 2003). Geometry of the slab surface at depths less than 50 km is also based on reflection/refraction studies (e.g., Sallerés et al., 2001).

our interpretation of the position of the slab surface (see below). Beneath Nicaragua, earthquakes extend to 200 km depth. Regional seismological observations (Protti et al., 1995) suggest the Cocos plate dips steeply (up to 84°) beneath Nicaragua, but this steep dip may be an overestimate, as the earthquake locations are largely controlled by distant seismographs in Costa Rica, a configuration, which can lead to severe biases in slab geometry (McLaren and Frohlich, 1985). Beneath central Costa Rica, where local networks provide good control, the EHB locations show a similar pattern as those of Protti et al. (1995) or Husen et al. (2003), but with more scatter. For this cross section we base the slab surface primarily on the teleseismic data set in Nicaragua, and the regional data set in Costa Rica. Both the dip of the subducting Cocos plate and the maximum earthquake depth decrease to the southeast. Beneath central Costa Rica, the Cocos plate subducts at ∼45° and earthquakes extend to ∼125 km depth. Beneath SE Costa Rica, where the Cocos Ridge is being subducted, there are no earthquakes deeper than ∼60 km (Protti et al., 1995; Husen et al., 2003); we assume a constant slab dip of 30° for depths >50 km. Beneath northern Costa Rica, Wadati-Benioff zone earthquakes suggest the subducted Cocos plate is torn at depths >70 km. This slab tear, the Quesada Sharp Contortion (QSC), separates steeper slab dips to the northeast from shallower slab dips to the southwest (Protti et al., 1995) (Fig. 1). The QSC projects updip to the Fisher Ridge, a propagator on the Cocos plate.

Stoiber and Carr (1973) divided the Central American volcanic arc into seven segments based on changes in the position and strike of the volcanic front. Several of these segments occur within Costa Rica – Nicaragua (Fig. 1). Geochemical studies of mafic lavas reveal dramatic variations in inferred arc magma sources and melting processes both along the strike of the arc (Carr et al., 1990; Feigenson and Carr, 1993; Leeman et al.,

1994) and across the arc (Walker et al., 1995). Arc lavas are generated by both decompression melting and flux melting triggered by fluids derived from the subducted Cocos plate (Carr et al., 1990; Feigenson and Carr, 1993; Leeman et al., 1994; Walker et al., 1995).

A number of geochemical studies have assessed the role of subducted material in generating arc lavas by comparing the concentration of fluid-mobile elements (e.g., B, Ba) to the concentration of immobile elements (e.g., La, Zr) in arc basalts. Volcanic front lavas contain up to 0.5% subducted sediment, or a fluid derived from the subducted sediment (Carr et al., 1990). Ratios such as B/La, Ba/La, and $^{10}Be/Be$ indicate that the subducted slab signal is greatest in the Nicaragua arc where the slab dips steeply and is at a minimum in the Costa Rica arc (Carr et al., 1990; Morris et al., 1990; Leeman et al., 1994). The rapid along-strike change in arc geochemistry occurs close to the border between Nicaragua and Costa Rica where the position of the volcanic front shifts, some 150 km northwest of the major change in slab geometry represented by the Quesada Sharp Contortion (Fig. 1). Patino et al. (2000) demonstrated that regional variations in arc lava geochemistry reflect differences in the sediment slab flux whereas local variations can be linked to variable incorporation of subducted hemipelagic sediments. Rüpke et al. (2002) proposed that the stronger slab signal in Nicaraguan arc lavas reflects greater amounts of fluid released from the dehydration of more extensively serpentinized slab mantle. The Nicaraguan slab is marked by an unusually well developed low-V_p wave guide (2.5–6 km thick, $14.5 \pm 2.2\%$ slow) at 100–150 km depth that is interpreted to reflect subducted crust containing >5 wt.% H_2O (Abers et al., 2003). This observation supports the unusually hydrated nature of the subducting Cocos plate beneath Nicaragua that probably results from extensive hydration along outer-rise faults and possibly updip fluid flow (Abers et al., 2003; Ranero et al., 2003).

Several ideas have been proposed to explain the large along-strike variations in both slab seismicity and arc geochemistry including hypotheses linked to the Cocos Ridge (Protti et al., 1995), variable plume flux (Herrstrom et al., 1995), a proposed slab window (Johnston and Thorkelson, 1997; Husen et al., 2003), plate age gradients (Protti et al., 1995), and slab dip (e.g., Carr et al., 1990). We test here the importance of the latter two effects, both of which should manifest themselves through changes in the thermal regime of the slab and overlying wedge. The changes can be predicted to be small at the slab surface, where the effects of increasing velocity and decreasing plate age towards the southeast are expected to offset each other. However, because the incoming lithosphere is relatively young, we expect significant differences in the thermal structure of the deeper oceanic crust and oceanic mantle of the subducting plate. In this paper we use a modeling approach to help determine whether changes in the thermal structure along the arc can explain the observed variations in seismicity and arc magmatism or if other explanations are required, such as the amount of sediment subduction or the extent to which the incoming crust and mantle are hydrated. Specifically, we assess the extent to which variations exist in dehydration and melting of subducted sediment, altered oceanic crust, and possibly deeper parts of the downgoing plate.

3. Thermal modeling

We constructed four two-dimensional finite-element thermal models across the Costa Rica – Nicaragua subduction zone (see profiles in Fig. 1) following the general modeling approach described by Van Keken et al. (2002). We present steady-state solutions. For each transect, we used seismic reflection–refraction studies (Christeson et al., 1999; Ranero et al., 2000; Sallerés et al., 2001) to define the shallow geometry of the subducting plate and observed Wadati-Benioff zone seismicity (Protti et al., 1995) to define the deeper geometry (Fig. 2).

The models have a length of 300 km and a depth that varies from 400 km for the steeply dipping Nicaragua model to 260 km for the more shallowly dipping SE Costa Rica model. Our finite-element models consist of more than 65,000 triangular elements corresponding to an average resolution of less than 1 km with additional grid refinement in the thermal boundary layers of the model. We impose the following boundary conditions: (i) The surface temperature is fixed at 0 °C. (ii) The temperature along the base of the 95 km thick subducting plate is fixed at 1450 °C. (iii) For the trench-side boundary condition, temperatures in the incoming lithosphere were defined by an oceanic error-function geotherm based on the age of the Cocos plate at the trench, which is 24 Ma for Nicaragua (A–A′)

and NW Costa Rica (B–B′), 18 Ma for central Costa Rica (C–C′), and 15 Ma for SE Costa Rica (D–D′) (Barckhausen et al., 2001). (iv) For the arc-side boundary condition, temperatures are defined by a continental geotherm that yields a surface heat flux of 65 mW/m^2 (average global continental heat flow, Pollack et al., 1993).

The velocity field in the subducting plate is defined kinematically. We use DeMets et al. (1994) NUVEL-1A plate motions to define the transect-parallel subduction rate, resulting in rates of 79 mm/year for Nicaragua, 83 mm/year for NW Costa Rica, 87 mm/year for central Costa Rica, and 88 mm/year for SE Costa Rica. The subducting plate drives the flow in the mantle–wedge. We define the top of the mantle–wedge, which is the base of the overlying rigid lithosphere, to lie at 50 km depth (e.g., Peacock and Wang, 1999). We use no-slip boundary conditions at both the top and slab side of the wedge, except for a 1 km segment at the corner point, which helps the stability and accuracy of the temperature solution (Van Keken et al., 2002). We investigate the thermal effects of two different mantle–wedge viscosity models: (i) constant viscosity (isoviscous) and (ii) temperature- and stress-dependent viscosity (olivine rheology) (Van Keken et al., 2002).

Our models incorporate radiogenic heating within the continental crust and shear heating along the plate interface. Radiogenic heating in the upper continental crust (0–15 km depth) and lower continental crust (15–30 km depth) produces 1.07×10^{-6} and 2.30×10^{-7} W/m^3, respectively, which accounts for 0.026 W/m^2 (40%) of the 0.065 W/m^2 upper-plate surface heat flow.

The rate of shear heating (Q_{sh}) along the plate interface is defined by the product of the convergence

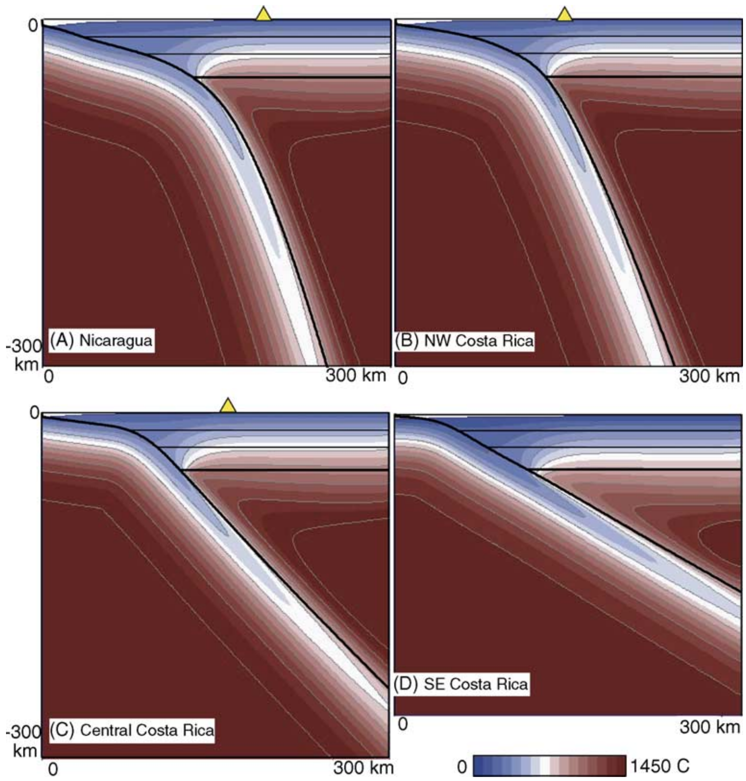

Fig. 3. Calculated thermal structure for four different transects across Central American subduction zone. Isoviscous mantle–wedge rheology; shear stress (τ) along plate interface = 10 MPa. Bold lines represent top of subducting slab and top of convecting mantle–wedge. Thin horizontal lines represent mid-crust (15 km depth) and Moho (30 km) of overriding plate. Contour interval = 100 °C. (A) Nicaragua, (B) NW Costa Rica, (C) Central Costa Rica, (D) SW Costa Rica.

rate (V) and shear stress (τ). Interface shear stresses, and therefore the rate of shear heating, represent a source of considerable uncertainty in subduction-zone thermal models (Peacock, 1996, 2003). Surface heat flow measurements (e.g., Hyndman and Wang, 1995; von Herzen et al., 2001), trench topography (Zhong and Gurnis, 1994), and upper-plate stress fields (Wang et al., 1995) suggest interface shear stresses in subduction zones lie in the range of 0–40 MPa. We lack surface heat flow measurements from the Nicaragua – Costa Rica forearc that could be used to constrain the rate of shear heating. In this paper, we present thermal models assuming a constant shear stress along the plate interface of 10 MPa down to a depth of 50 km. The temperature solution is obtained without considering adiabatic (de)compression and therefore underestimates the temperature at depth. The P–T paths plotted in Figs. 5–7 have been obtained after a posteriori addition of an adiabatic temperature gradient of 0.3 K/km.

4. Predicted thermal structure

The calculated thermal structure for the four Central American subduction-zone transects are depicted in Fig. 3 (isoviscous mantle–wedge rheology) and Fig. 4 (olivine mantle–wedge rheology). The rapid 80–90 mm/year subduction of oceanic lithosphere results in isotherms within and near the subducting slab being depressed hundreds of kilometers into the mantle. Rapid subduction chills the subduction-zone forearc while temperatures within the mantle–wedge remain high as a result of the corner flow induced by the subducting plate. For the isoviscous mantle–wedge rheology, predicted maximum temperatures beneath the volcanic front range from ∼1400 °C beneath Nicaragua (Cerro Negro) to ∼1150 °C beneath SE Costa Rica (Fig. 3). These results indicate that the temperatures below the volcanic front, with the exception of Nicaragua, are generally quite cool. Higher temperatures are obtained when using a more realis-

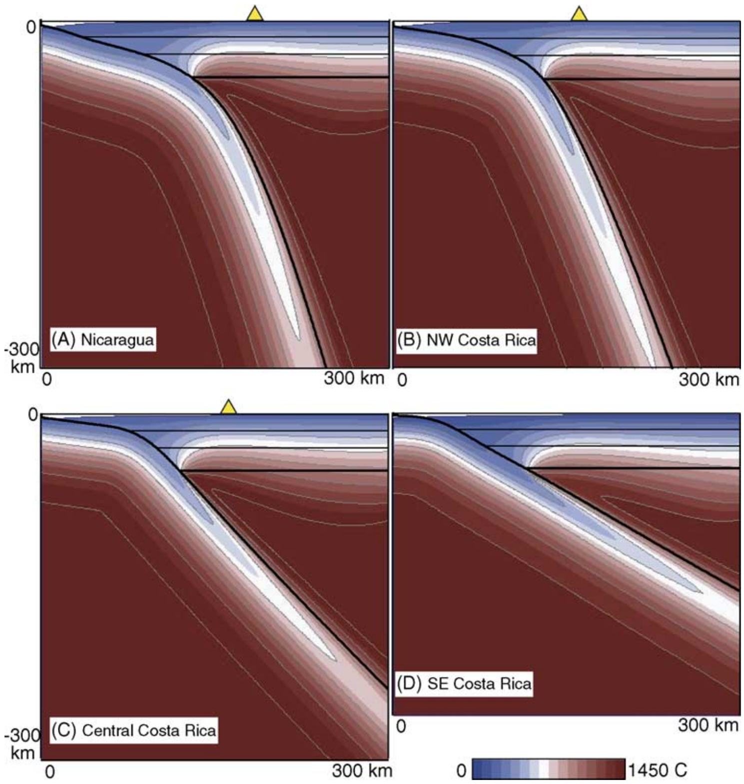

Fig. 4. Same as Fig. 3 with olivine mantle–wedge rheology.

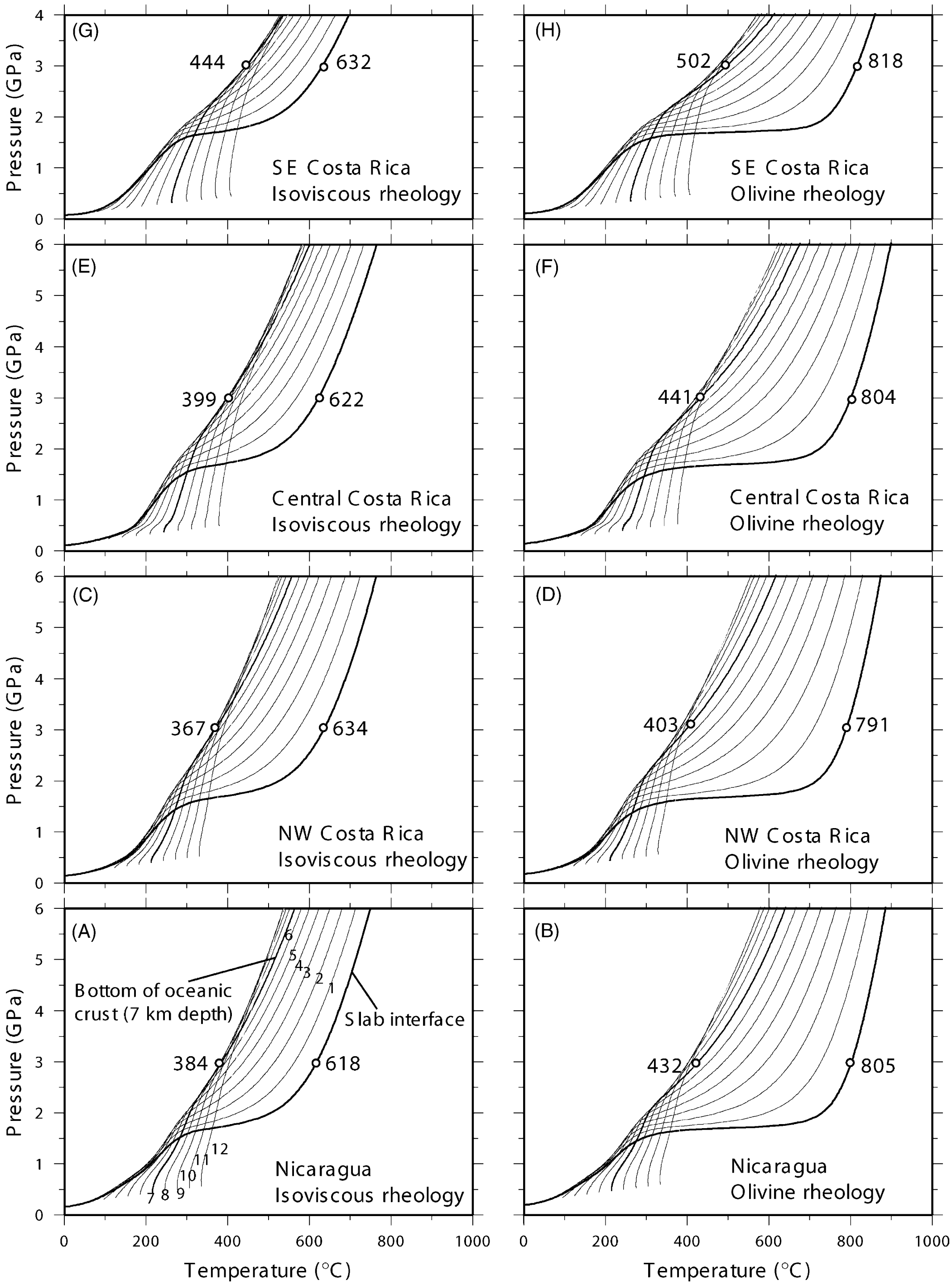

Fig. 5. *P–T* paths for subducting lithosphere beneath Central America calculated using isoviscous and olivine mantle–wedge rheology. Paths are depicted for a rock located at the top of the subducting plate and at 1 km intervals within the subducting plate down to 12 km below the interface. Bold lines depict *P–T* paths followed by top and bottom of the 7 km thick subducting oceanic crust. Shear stress (τ) along plate interface = 10 MPa. (A) Nicaragua, isoviscous rheology; (B) Nicaragua, olivine rheology; (C) NW Costa Rica, isoviscous rheology; (D) NW Costa Rica, olivine rheology; (E) Central Costa Rica, isoviscous rheology; (F) Central Costa Rica, olivine rheology; (G) SE Costa Rica, isoviscous rheology; (H) SE Costa Rica, olivine rheology.

tic temperature- and stress-dependent rheology based on a creep law for dry olivine (Karato and Wu, 1993; Van Keken et al., 2002). In this case the cross sections through NW and Central Costa Rica indicate that the hot mantle–wedge extends to just under the volcanic front (Fig. 4).

Differences among predicted slab interface *P*–*T* paths for the four Costa Rica – Nicaragua models are relatively small. For the isoviscous mantle–wedge rheology, predicted temperatures along the slab interface are ∼620 °C at $P = 3$ GPa (100 km depth) for all four transects (Fig. 5A). For the olivine mantle–wedge rheology predicted temperatures along the slab interface are significantly warmer, ∼800 °C at 3 GPa (Fig. 5B). In the mantle–wedge, material dragged down by the subducting plate is replaced by even hotter material in the olivine rheology calculations, as compared to the isoviscous rheology, resulting in warmer slab interface temperatures. Calculated *P*–*T* paths for rocks within the subducting plate are less sensitive to the rheology of the mantle–wedge. For example, beneath NW Costa Rica, predicted temperatures at 3 GPa at the base of the 7 km thick subducting oceanic crust are 367 and 403 °C for an isoviscous and olivine mantle–wedge rheology, respectively (Fig. 5). The effect of the hydrothermally cooled upper portion of the oceanic crust in model C–C′ extends along the slab interface only to shallow depths (less than 15 km); the high temperature gradient in the interface region causes quick recovery of the departure from the conductive cooling model.

5. Dehydration and partial melting reactions

To predict the mineralogy and regions of dehydration within the subducting crust and mantle, we combine calculated slab *P*–*T* paths with phase diagrams constructed for mafic and ultramafic compositions (Fig. 6) (Hacker et al., 2003a). The mafic phase diagram was constructed for mid-ocean ridge basalt using field-based petrological studies and thermodynamic calculations of key facies-bounding metamorphic reactions. The ultramafic phase diagram was constructed for depleted harzburgite using thermodynamic calculations and the results of high-pressure experiments, see Hacker et al. (2003a) for a detailed description of the approach used to construct both phase diagrams. It is important to note that the upper oceanic crust of the sub-

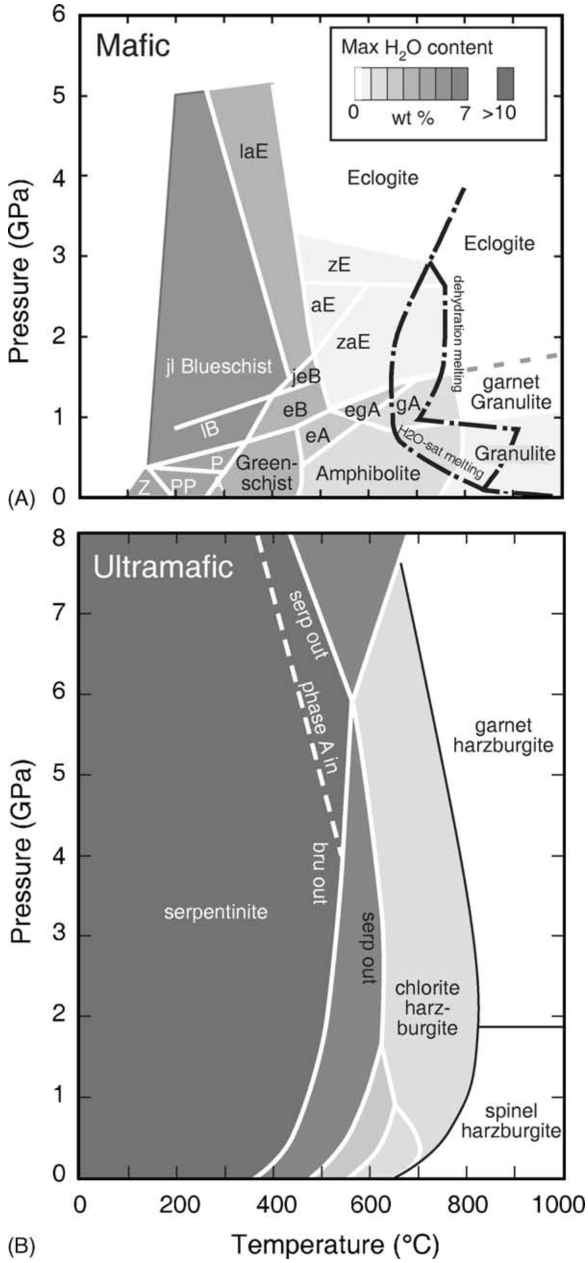

Fig. 6. Phase diagrams constructed for (A) mafic (mid-ocean ridge basalt) and (B) depleted ultramafic (harzburgite) compositions (after Hacker et al., 2003a). Gray shading is proportional to H_2O content. Black dash-dot lines are partial melting reactions. Metamorphic facies abbreviations: A, amphibolite; B, blueschist; PA, prehnite–actinolite; PP, prehnite–pumpellyite; Z, zeolite. Mineral abbreviations: a, amphibole; bru, brucite; e, epidote; g, garnet; j, jadeite; l, lawsonite; serp, serpentine (antigorite); z, zoisite.

ducting slab, which is composed of partially hydrated fine-grained rocks, undergoes near-equilibrium phase changes to the mineral assemblages shown in Fig. 6. In contrast, the mostly dry, coarse-grained lower oceanic crust likely transforms to higher pressure mineral assemblages only after considerable overstepping beyond the equilibrium boundaries (Hacker, 1996; Hacker et al., 2003a).

For an isoviscous mantle–wedge, calculated slab *P–T* paths remain below the solidus and no partial melting of the subducting oceanic crust is predicted. For an olivine mantle–wedge rheology, calculated *P–T* paths for the slab interface cross the H_2O-saturated mafic solidus at pressures of 2–3 GPa (Fig. 7A), suggesting that the uppermost 500 m of the subducting oceanic crust may undergo partial melting at depths of 65–100 km. The amount of partial melting will be <1 vol.% at the H_2O-saturated solidus because the porosity, and therefore the amount of free H_2O available to trigger melting, is expected to be <1 vol.% at these *P–T* conditions and the solubility of H_2O in the magma is large at these pressures. More significant amounts of partial melting may occur at ∼100 km depth where calculated slab interface *P–T* paths exceed the fluid-absent (dehydration) solidus by several tens of degrees. Calculated slab interface *P–T* paths exceed the wet solidus for sedimentary bulk compositions, suggesting that partial melting of subducted sediments may occur.

Calculated *P–T* paths for deeper portions of the subducting oceanic crust exhibit larger differences among the four profiles than *P–T* paths for the slab surface, but

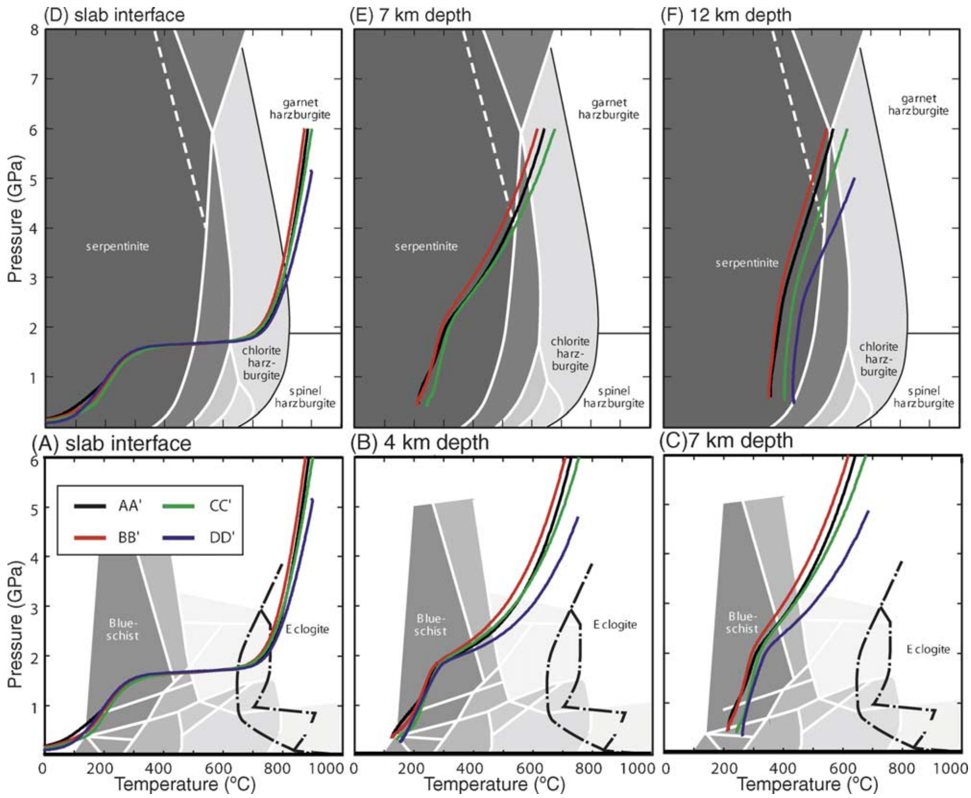

Fig. 7. Calculated *P–T* paths for subducting oceanic crust and mantle beneath Nicaragua (profile A–A′, black), NW Costa Rica (profile B–B′, red), central Costa Rica (profile C–C′, green), and SE Costa Rica (profile D–D′, blue) superimposed on mafic (panels A–C) and ultramafic phase diagrams (panels D–F). Olivine mantle–wedge rheology, shear stress = 10 MPa. (A) Slab interface *P–T* paths (top of subducting oceanic crust). (B) *P–T* paths for rocks located 4 km beneath slab interface. (C) *P–T* paths for rocks located 7 km beneath slab interface (approximate base of subducting oceanic crust). (D) Slab interface *P–T* paths (representing conditions at the base of mantle–wedge), (E) *P–T* paths for top of the mantle section at 7 km depth (profile A–A′ through C–C’ only) (F) *P–T* paths for mantle rocks located 12 km beneath slab interface.

the maximum difference at any pressure is still less than ~100 °C (Fig. 7B and C). The subducting crust beneath SE Costa Rica is the warmest because the incoming lithosphere is the youngest (Fig. 7B and C). The bulk of the subducting oceanic crust enters the lawsonite-amphibole eclogite stability field at 1.6–3 GPa with deeper portions of the subducting crust entering at pressures of 3–3.5 GPa.

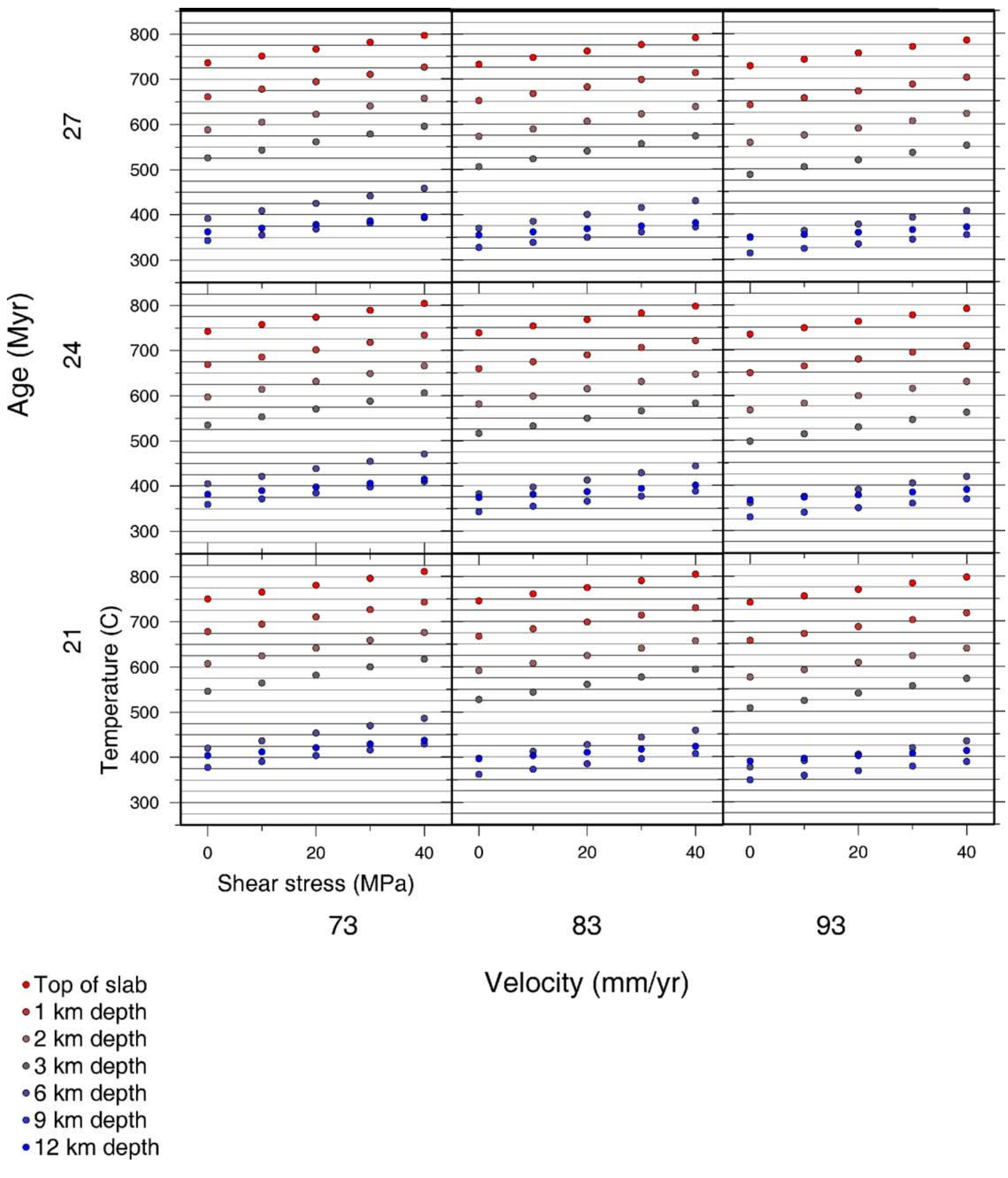

Fig. 8. Sensitivity analysis showing the departures of the predicted temperature at various depths in the subducting plate at a pressure of 3 GPa for the NW Costa Rica model (profile B–B′) as a function of small variations in subduction velocity, age of the lithosphere, and rate of shear heating.

Calculated *P*–*T* paths followed by subducting oceanic mantle are significantly cooler beneath Nicaragua and NW Costa Rica (Fig. 7E and F), primarily because the age of the incoming lithosphere and the dip of the subducting slab increase to the northeast. At 3 GPa, predicted temperatures at a point 12 km below the slab interface within the subducting mantle range from 370 °C beneath Nicaragua and NW Costa Rica to 460 °C beneath SE Costa Rica (Fig. 7F). Beneath SE Costa Rica, hydrated parts of the subducting mantle will have undergone significant dehydration to chlorite harzburgite by ∼160 km (5 GPa). In contrast, hydrated oceanic mantle subducted beneath Nicaragua and Costa Rica may still contain substantial amounts of H_2O at depths greater than 240 km (>8 GPa). In contrast, chlorite harzburgite in the overlying mantle–wedge is predicted to dehydrate at ∼115 km depth (3.8 GPa) in all four profiles (Fig. 7D).

6. Sensitivity analysis

The calculated thermal structure and slab *P*–*T* paths are relatively insensitive to modest variations in the convergence rate, age of the incoming lithosphere, and interface shear stress. We evaluated the sensitivity of our calculations by systematically varying these parameters for the NW Costa Rica model with non-Newtonian olivine rheology in the mantle–wedge (Fig. 8). The temperatures are shown without taking the adiabatic gradient into account. At 3 GPa (100 km depth), the calculated slab interface temperature is 754 °C for the preferred values for convergence rate (83 mm/year), age of the incoming lithosphere (24 Ma), and interface shear stress (10 MPa). Varying the convergence rate from 73 to 93 mm/year results in calculated slab interface temperatures ranging from 758 to 748 °C. Varying the age of the incoming lithosphere from 21 to 27 Ma results in calculated slab interface temperatures ranging from 761 to 747 °C. Varying the interface shear stress from 0 to 40 MPa results in calculated slab interface temperatures ranging from 739 to 797 °C. Calculated temperatures within the upper few kilometers of the subducting plate vary by similar amounts (Fig. 8). Decreasing the depth to which shear heating extends from 50 to 30 km results in calculated slab interface temperatures that are 10 °C cooler at 2 GPa.

7. Conclusions

Thermal models constructed across the Nicaragua – Costa Rica subduction zone reveal only minor along-strike variations in the calculated thermal structure. This suggests that observed along-strike variations in the distribution of Wadati-Benioff earthquakes and arc geochemistry are more likely related to regional variations in slab stresses, sediment subduction, crustal structure and the distribution of hydrous minerals in the incoming lithosphere (e.g., Rüpke et al., 2002; Abers et al., 2003; Ranero et al., 2003). For an olivine mantle–wedge rheology, calculated slab *P*–*T* paths intersect the H_2O-saturated mafic solidus, such that subducted sediment and the uppermost subducting oceanic crust may undergo partial melting at depths of 65–100 km. The bulk of the subducting oceanic crust is predicted to transform to lawsonite-amphibole eclogite at depths of 60–100 km with deeper portions of the subducting crust transforming at greater depths. Hydrous minerals in the subducting oceanic mantle may persist to greater depth.

Acknowledgements

We gratefully acknowledge NSF support to Peacock, Van Keken, Hacker and Abers for this research through the CSEDI program. We thank Sue Bilek and Heather DeShon for providing early access to their Costa Rica seismicity data sets. We thank Susan Schwartz and James Condor for their constructive reviews.

References

Abers, G.A., Plank, T., Hacker, B.R., 2003. The wet Nicaraguan slab. Geophys. Res. Lett. 30, 1098, doi:10.1029/2002GL015649.

Barckhausen, U., Ranero, C.R., von Huene, R., Cande, S.C., Roeser, H.A., 2001. Revised tectonic boundaries in the Cocos Plate off Costa Rica: implications for the segmentation of the convergent margin and for plate tectonics models. J. Geophys. Res. 106, 19207–19220.

Carr, M.J., Feigenson, M.D., Bennett, E.A., 1990. Incompatible element and isotopic evidence for tectonic control of source mixing and melt extraction along the Central American arc. Contrib. Mineral. Petrol. 105, 369–380.

Christeson, G.L., McIntosh, K.D., Shipley, T.H., Flueh, E.R., Goedde, H., 1999. Structure of the Costa Rica convergent margin, offshore Nicoya Peninsula. J. Geophys. Res. 104, 25443–25468.

DeMets, C., 2001. A new estimate for present-day Cocos–Caribbean Plate motion; implications for slip along the Central American volcanic arc. Geophys. Res. Lett. 28, 4043–4046.

DeMets, C., Gordon, R.G., Argus, D.F., Stein, S., 1994. Effect of recent revisions to the geomagnetic reversal timescale on estimates of current plate motions. Geophys. Res. Lett. 21, 2191–2194.

DeShon, H.R., Schwartz, S.Y., Bilek, S.L., Dorman, L.M., Gonzalez, V., Protti, J.M., Flueh, E.R., Dixon, T.H., 2003. Seismogenic zone structure of the southern Middle America trench, Costa Rica. J. Geophys. Res. 108, 2491, doi: 10.1029/2002JB002294.

Engdahl, E.R., van der Hilst, R., Buland, R., 1998. Global teleseismic earthquake relocation with improved travel times and procedures for depth determination. Bull. Seismol. Soc. Am. 88, 722–743.

Feigenson, M.D., Carr, M.J., 1993. The source of Central American lavas: inferences from geochemical inverse modeling. Contrib. Mineral. Petrol. 113, 226–235.

Fisher, A.T., Stein, C.A., Harris, R.N., Wang, K., Silver, E.A., Pfender, M., Hutnak, M., Cherkaoui, A., Bodzin, R., Villinger, H., 2003. Abrupt thermal transition reveals hydrothermal boundary and role of seamounts within Cocos Plate. Geophys. Res. Lett. 30, 150, doi:10.1029/2002GL016766.

Hacker, B.R., 1996. Eclogite formation and the rheology, buoyancy, seismicity, and H_2O content of oceanic crust. In: Bebout, G.E., Scholl, D.W., Kirby, S.H., Platt, J.P. (Eds.), Subduction: Top to Bottom. Geophysical Monograph Ser. American Geophysical Union, Washington, DC, pp. 337–346.

Hacker, B.R., Abers, G.A., Peacock, S.M., 2003a. Subduction factory – 1. Theoretical mineralogy, densities, seismic wave speeds, and H_2O contents. J. Geophys. Res. 108, 2029, doi:10.1029/2001JB001127.

Hacker, B.R., Peacock, S.M., Abers, G.A., Holloway, S.D., 2003b. Subduction factory – 2. Are intermediate-depth earthquakes in subducting slabs linked to metamorphic dehydration reactions? J. Geophys. Res. 108, 2030, doi:10.1029/2001JB001129.

Herrstrom, E.A., Reagan, M.K., Morris, J.D., 1995. Variations in lava composition associated with flow of asthenosphere beneath southern Central America. Geology 23, 617–620.

Husen, S., Quintero, R., Kissling, E., Hacker, B.R., 2003. Subduction zone structure and magmatic processes beneath Costa Rica as constrained by local earthquake tomography and petrologic modeling. Geophys. J. Int. 155, 11–32.

Hyndman, R.D., Wang, K., 1995. The rupture zone of Cascadia great earthquakes from current deformation and the thermal regime. J. Geophys. Res. 100, 22133–22154.

Johnston, S.T., Thorkelson, D.J., 1997. Cocos-Nazca slab window beneath Central America. Earth Planet. Sci. Lett. 146, 465–474.

Karato, S., Wu, P., 1993. Rheology of the upper mantle: a synthesis. Science 260, 771–778.

Kirby, S.H., Engdahl, E.R., Denlinger, R., 1996. Intraslab earthquakes and arc volcanism: dual physical expressions of crustal and uppermost mantle metamorphism in subducting slabs. In: Bebout, G.E., Scholl, D.W., Kirby, S.H., Platt, J.P. (Eds.), Subduction: Top to Bottom. Geophysical Monograph Ser. American Geophysical Union, Washington, DC, pp. 195–214.

Kimura, G., Silver, E.A., Plum, P., et al., 1997. Proceedings of the ODP, Init. Repts., 170, College Station, TX (Ocean Drilling Program).

Langseth, M.G., Silver, E.A., 1996. The Nicoya convergent margin—a region of exceptionally low heat flow. Geophys. Res. Lett. 23, 891–894.

Leeman, W.P., Carr, M.J., Morris, J.D., 1994. Boron geochemistry of the Central American Volcanic Arc: constraints on the genesis of subduction-related magmas. Geochim. Cosmochim. Acta 58, 149.

McLaren, J.P., Frohlich, C., 1985. Model calculations of regional network locations for earthquakes in subduction zones. Bull. Seismol. Soc. Am. 75, 397–413.

Morris, J., Leeman, W.P., Tera, F., 1990. The subducted component in island arc lavas: constraints from Be isotopes and B–Be systematics. Nature 344, 31–36.

Morris, J., Valentine, R., Harrison, T., 2002. ^{10}Be imaging of sediment accretion and subduction along the northeast Japan and Costa Rica convergent margins. Geology 30, 59–62.

Newman, A.V., Schwartz, S.Y., Gonzalez, V., DeShon, H.R., Protti, J.M., Dorman, L., 2002. Along-strike variability in the updip limit of the seismogenic zone below Nicoya Peninsula Costa Rica. Geophys. Res. Lett. 29 (38), 1–4.

Norabuena, E., Dixon, T.H., Schwartz, S., DeShon, H., Newman, A., Protti, M., Gonzalez, V., Dorman, L., Flueh, E.R., Lundgren, P., Pollitz, F., Sampson, D., 2004. Geodetic and seismic constraints on some seismogenic zone processes in Costa Rica. J. Geophys. Res. 109, B11403, doi:10.1029/2003JB002931.

Patino, L.C., Carr, M.J., Feigenson, M.D., 2000. Local and regional variations in Central American arc lavas controlled by variations in subducted sediment input. Contrib. Mineral. Petrol. 138, 265–283.

Peacock, S.M., 1996. Thermal and petrologic structure of subduction zones. In: Bebout, G.E., Scholl, D.W., Kirby, S.H., Platt, J.P. (Eds.), Subduction: Top to Bottom. Geophysical Monograph Ser. American Geophysical Union, Washington, DC, pp. 119–133.

Peacock, S.M., Wang, K., 1999. Seismic consequences of warm versus cool subduction zone metamorphism: examples from northeast and southwest Japan. Science 286, 937–939.

Peacock, S.M., 2003. Thermal structure and metamorphic evolution of subducting slabs. In: Eiler, J.M. (Ed.), Inside the Subduction Factory. Geophysical Monograph Ser. American Geophysical Union, Washington, DC, pp. 7–22.

Pollack, H.N., Hurter, S.J., Johnson, J.R., 1993. Heat flow from the Earth's interior: analysis of the global data set. Rev. Geophys. 31, 267–280.

Protti, M., Guendel, F., McNally, K., 1995. Correlation between the age of the subducting Cocos plate and the geometry of the Wadati-Benioff zone under Nicaragua and Costa Rica. Geol. Soc. Am. Spec. Paper 295, 309–326.

Ranero, C.R., von Huene, R., 2000. Subduction erosion along the Middle America convergent margin. Nature 404, 748–752.

Ranero, C.R., von Huene, R., Flueh, E., Duarte, M., Baca, D., McIntosh, K., 2000. A cross section of the convergent Pacific margin of Nicaragua. Tectonics 19, 335–357.

Ranero, C.R., Phipps Morgan, J., McIntosh, K., Reichert, C., 2003. Bending-related faulting and serpentinization at the Middle America trench. Nature 425, 367–373.

Rüpke, L.H., Morgan, J.P., Hort, M., Connolly, J.A.D., 2002. Are the regional variations in Central American arc lavas due to differing basaltic versus peridotitic slab sources of fluids? Geology 30, 1035–1038.

Sallerés, V., Dañobeitia, J.J., Flueh, E.R., 2001. Lithospheric structure of the Costa Rican Isthmus: effects of subduction zone magmatism on an oceanic plateau. J. Geophys. Res. 106, 621–643.

Silver, E.A., 2000. Leg 170: Synthesis of fluid-structural relationships of the Pacific margin of Costa Rica. In: Silver, E.A., Kimura, G., Shipley, T.H. (Eds.), Proc. ODP, Sci. Results, vol. 170, pp. 1–11.

Stoiber, R.E., Carr, M.J., 1973. Quaternary volcanic and tectonic segmentation of Central America. Bull. Volcanol. 37, 304–325.

Van Keken, P.E., Kiefer, B., Peacock, S., 2002. High resolution models of subduction zones: implications for mineral dehydration reactions and the transport of water into the deep mantle. Geochem. Geophys. Geosyst. 3, doi: 10.1029/2001GC000256.

von Herzen, R., et al., 2001. A constraint on the shear stress at the Pacific-Australian plate boundary from heat flow and seismicity at the Kermadec forearc. J. Geophys. Res. 106, 6817–6833.

von Huene, R., Scholl, D.W., 1991. Observations at convergent margins concerning sediment subduction, subduction erosion, and the growth of continental crust. Rev. Geophys. 29, 279–316.

von Huene, R., Ranero, C.R., Weinrebe, W., Hinz, K., 2000. Quaternary convergent margin tectonics of Costa Rica, segmentation of the Cocos plate, and Central American volcanism. Tectonics 19, 314–334.

von Huene, R., et al., 1995. Morphotectonics of the Pacific convergent margin of Costa Rica. Geol. Soc. Amer. Spec. Paper, 295: 291–307.

Walker, J.A., Carr, M.J., Ward, R.L., 1995. Abrupt change in magma generation processes across the Central American arc in southeastern Guatemala: Flux-dominated melting near the base of the wedge to decompression melting near the top of the wedge. Contrib. Mineral. Petrol. 120, 378–390.

Walther, C.H., Bialas, J., Flueh, E.R., 2000. Crustal structure of the Cocos Ridge off Costa Rica-preliminary results from a seismic wide-angle experiment, EOS. Trans. Am. Geophys. Un., Fall Meet. Suppl., 81.

Wang, K., Mulder, T., Rogers, G.C., Hyndman, R.D., 1995. Case for very-low coupling stress on the Cascadia subduction fault. J. Geophys. Res. 100, 12907–12918.

Zhong, S.J., Gurnis, M., 1994. Controls on trench topography from dynamic-models of subducted slabs. J. Geophys. Res. 99, 15683–15695.